



## SECOND LAW BASED THERMODYNAMIC ANALYSIS OF COMPRESSION-ABSORPTION CASCADE REFRIGERATION CYCLES

Canan CIMSIT\*, İlhan Tekin OZTURK\*\* and Murat HOSOZ\*\*

\* Golcuk Vocational School of Higher Education, Kocaeli University, 41650 Golcuk, Turkey

\*\* Department of Mechanical Engineering, Kocaeli University, Umuttepe Campus, 41380 Kocaeli, Turkey

(Geliş Tarihi: 13.03.2013, Kabul Tarihi: 08.07.2013)

**Abstract:** In this study, energy and exergy analysis of compression-absorption cascade refrigeration cycles were performed. In order to determine the best suitable working pair in the absorption section of the cascade refrigeration system, LiBr-H<sub>2</sub>O and NH<sub>3</sub>-H<sub>2</sub>O pairs were compared by considering only R134a in the vapour compression section. In the case of using LiBr-H<sub>2</sub>O fluid couple in the absorption section of cascade refrigeration cycles, the coefficient of performance (*COP*) is 27% higher and total exergy destruction rate is 20% lower compared with the case of using NH<sub>3</sub>-H<sub>2</sub>O fluid couple. Based on these results, the first and second law thermodynamic analyses were carried out for different working temperatures of the system components by using only LiBr-H<sub>2</sub>O in the absorption section and using various refrigerants, namely NH<sub>3</sub>, R134a, R410A and CO<sub>2</sub>, in the vapor compression section. The results show that the *COP* of the cascade system increases by increasing the generator and evaporator temperatures, while it decreases by increasing the condenser and absorber temperatures. However, the exergetic efficiency decreases with increasing generator, absorber and condenser temperatures. Moreover, it was determined that NH<sub>3</sub>/LiBr-H<sub>2</sub>O cascade cycle has the best thermodynamic performance, while CO<sub>2</sub>/LiBr-H<sub>2</sub>O cascade cycle has substantially poorer performance than this cycle.

**Keywords:** Refrigeration; Absorption; Cascade; Coefficient of performance; Exergetic efficiency

## BUHAR SIKIŞTIRMALI-ABSORBSİYONLU KASKAD SOĞUTMA ÇEVİRİMLERİNİN İKİNCİ KANUN ANALİZİ

**Özet:** Bu çalışmada buhar sıkıştırma-absorbsiyonlu kaskad soğutma çevrimlerinin enerji ve ekserji analizi yapılmıştır. Kaskad soğutma çevriminin absorbsiyon kısmında en uygun akışkan çiftini belirlemek için buhar sıkıştırma kısmında sadece R134a soğutucu akışkanı kullanımı dikkate alınarak LiBr-H<sub>2</sub>O ve NH<sub>3</sub>-H<sub>2</sub>O çiftleri karşılaştırılmıştır. Kaskad soğutma sistemlerinin absorbsiyonlu kısmında LiBr-H<sub>2</sub>O akışkan çiftinin kullanılması durumunda NH<sub>3</sub>-H<sub>2</sub>O akışkan çiftine göre % 27 daha yüksek soğutma tesir katsayısı (STK) ve ikinci kanun analiz sonucuna göre % 20 daha düşük ekserji kayıpları elde edilmiştir. Bu sonuçlara dayanarak kaskad soğutma sistemlerinin absorbsiyonlu kısmında sadece LiBr-H<sub>2</sub>O akışkan çiftinin buhar sıkıştırma kısmında ise NH<sub>3</sub>, R-134a, R410A ve CO<sub>2</sub> soğutucu akışkanların kullanıldığı düşünülerek oluşturulan çevrimlerin sistem elemanlarının farklı çalışma sıcaklıklarına göre birinci ve ikinci kanun analizleri yapılmıştır. Bu analizlere göre kaskad çevriminin yoğunlaştırıcı ve absorber sıcaklığı arttıkça çevrimin STK değeri azalmakta, buna karşılık kaynatıcı ve buharlaştırıcı sıcaklığının artmasıyla da çevrimin STK değerinin artmakta olduğu tespit edilmiştir. Artan absorber, kaynatıcı ve kondenser sıcaklıklarında ekserji veriminin azaldığı görülmüştür. Ayrıca, CO<sub>2</sub>/LiBr-H<sub>2</sub>O kaskad çevrimi çok daha kötü performansa sahipken NH<sub>3</sub>/LiBr-H<sub>2</sub>O kaskad çevriminin en iyi termodinamik performansa sahip olduğu tespit edilmiştir.

**Anahtar Kelimeler:** Soğutma; Absorbsiyon; Kaskad; Performans katsayısı; Ekserji etkinliği

### NOMENCLATURE

<i>COP</i>	coefficient of performance	$\dot{m}$	mass flow rate [kg s <sup>-1</sup> ]
<i>e</i>	specific exergy [kJ kg <sup>-1</sup> ]	<i>P</i>	pressure [kPa]
$\dot{E}$	exergy flow rate [kW]	<i>s</i>	specific entropy [kJ kg <sup>-1</sup> K <sup>-1</sup> ]
<i>ECOP</i>	exergetic efficiency	$\dot{Q}$	heat flow rate [kW]
<i>f</i>	circulation ratio	<i>T</i>	temperature [K]
$\varepsilon$	effectiveness of the solution heat exchanger	$\dot{W}$	work flow rate or power of compressor [kW]
<i>h</i>	enthalpy [kJ kg <sup>-1</sup> ]	<i>x</i>	concentration

### Subscripts

<i>abs</i>	absorber or absorption system
<i>comp</i>	compressor
<i>con</i>	condenser
<i>cyclegen</i>	cycle general
<i>evap</i>	evaporator
<i>gen</i>	generator
<i>HX</i>	heat exchanger
<i>i</i>	input
<i>o</i>	output
<i>0</i>	ambient
<i>rev</i>	refrigerant expansion valve
<i>sev</i>	solution expansion valve
<i>she</i>	solution heat exchanger
<i>t</i>	total system
<i>vapor-comp</i>	vapor-compression

### INTRODUCTION

Nowadays, world energy consumption is increasing rapidly, and cooling systems account for a considerable fraction of this consumption. Because compression-absorption cascade refrigeration cycles use alternative thermal energy sources and industrial waste heat, these systems provide substantial electric energy savings as well as being environmentally friendly. There are many studies on the absorption refrigeration systems in the literature.

Joudi and Lafta (2001) developed a steady state computer simulation model to predict the performance of an absorption refrigeration system using LiBr-H<sub>2</sub>O as a working pair. Their model utilized mass and energy balances along with heat and mass transfer relationships for the cycle components. They determined a good agreement between the simulation results and manufacturer's data.

Florides *et al.* (2003) presented a method to evaluate the characteristics and performance of a single stage LiBr-H<sub>2</sub>O absorption machine. They compared the theoretical results with experimental ones obtained for a small unit, finding that the price of LiBr-H<sub>2</sub>O absorption refrigeration unit is higher than that of a similar capacity electric chiller.

Sozen (2001) investigated the effect of heat exchangers on the coefficient of performance (*COP*), exergetic coefficient of performance (*ECOP*), circulation rate and nondimensional exergy loss in each component for an absorption refrigeration system.

Talbi and Agnew (2000) performed an exergy analysis of a single-effect absorption refrigeration cycle using LiBr-H<sub>2</sub>O as the working fluid pair. They applied a design procedure to the absorption cycle, and performed an optimisation procedure that consists of determining the enthalpy, entropy, temperature, mass flow rate, heat transfer rate in each component, and *COP*.

Adewusi and Zubair (2004) performed the second law thermodynamic analysis of NH<sub>3</sub>-H<sub>2</sub>O absorption refrigeration systems. The entropy generation of each

component and the total entropy generation in the entire system as well as *COP* of the NH<sub>3</sub>-H<sub>2</sub>O absorption refrigeration systems were calculated from the thermodynamic properties of the working fluids for various operating conditions. They determined that the two-stage generator causes an entropy generation of more than 50% of the total entropy generation in the two-stage NH<sub>3</sub>-H<sub>2</sub>O absorption refrigeration systems.

Sencan *et al.* (2005) carried out an exergy analysis of a single-effect LiBr-H<sub>2</sub>O absorption system for cooling and heating applications. They evaluated the exergy loss, enthalpy, entropy, temperature, mass flow rate and heat rate in each component of the system. They found that the cooling and heating *COP* of the system increase slightly and the exergetic efficiency of the system decreases for both cooling and heating applications with increasing the heat source temperature.

Kilic and Kaynakli (2007) performed the first and second law thermodynamic analyses of a single-stage LiBr-H<sub>2</sub>O absorption refrigeration system under varying operating conditions. They determined that the performance of the absorption refrigeration system increases with increasing generator and evaporator temperatures, but decreases with increasing condenser and absorber temperatures. They also reported that the highest exergy loss occurs in the generator regardless of operating conditions, thus making the generator the most important component of the cycle.

Kaynakli and Yamankaradeniz (2007) performed the first and second law thermodynamic analyses of a single-stage absorption refrigeration cycle with LiBr-H<sub>2</sub>O as working fluid pair. They reported that the total entropy generation of the system decreases with increasing generator temperature.

Kaynakli and Kilic (2007) carried out a detailed thermodynamic analysis of the LiBr-H<sub>2</sub>O absorption refrigeration cycle. They investigated the influences of operating temperature and effectiveness of the heat exchanger on the thermal loads of the components, *COP* and efficiency ratio. They concluded that the solution heat exchanger increases the *COP* up to 44% while the refrigerant heat exchanger promotes the *COP* only by 2.8%.

Kaushik and Arora (2009) performed the energy and exergy analyses of single effect and series flow double effect LiBr-H<sub>2</sub>O absorption systems. They developed a computer program for the parametric investigation of these systems, and presented the effect of various parameters. Their results indicated that the *COP* of the double effect system is about 60–70% higher than that of the single effect system. The highest irreversibility occurs in the absorber in both systems when compared to other system components.

Rivera *et al.* (2010) carried out first and second law thermodynamic analyses of an experimental single-stage heat transformer operating with the LiBr-H<sub>2</sub>O mixture. Their results showed that the highest *COP*, external *COP* and *ECOP* values are obtained at the

highest solution concentrations (59%), meanwhile the improvement potential of the cycle and irreversibility remain almost constant against this parameter.

Misra *et al.* (2003) performed the thermoeconomic optimization of a single effect LiBr-H<sub>2</sub>O vapor absorption refrigeration system. They presented the application of the exergy-based thermoeconomic technique to optimize a single effect LiBr-H<sub>2</sub>O vapour absorption refrigeration system used for air-conditioning purposes.

Tarique and Siddiqui (1999) made a comparison between and the compression-absorption (combined) refrigeration system using NH<sub>3</sub>-NaSCN and the vapor compression refrigeration system using ammonia for the same operating conditions in terms of the economy and performance. They determined that the NH<sub>3</sub>-NaSCN system has significantly less capital and operating costs of the compressors compared with the system using ammonia.

Kairouani and Nehdi (2006) employed NH<sub>3</sub>-H<sub>2</sub>O fluid pair in the absorption section of the compression-absorption cascade refrigeration cycle, while used R717, R22 and R134a in the vapor compression section. They determined that their system had 37-54% higher COP values compared with conventional cycles operating under the same conditions.

Cimsit and Ozturk (2012) performed a first law analysis of compression-absorption cascade systems. They used LiBr-H<sub>2</sub>O and NH<sub>3</sub>-H<sub>2</sub>O fluid pairs in cascade absorption section along with R134a, R410a and NH<sub>3</sub> fluids in the vapor-compression section of cascade cycle. They reported that the COP obtained with the LiBr-H<sub>2</sub>O is higher than that obtained with NH<sub>3</sub>-H<sub>2</sub>O fluid pair for the same application. Moreover, they compared the cascade refrigeration cycles with mechanical vapor compression refrigeration systems, finding that cascade cycles require less electrical energy ranged between 48% and 52% compared with the other system to obtain the same amount refrigeration for the same conditions. This analysis is based on just the first law of thermodynamics, and did not consider CO<sub>2</sub> as a refrigerant in vapor compression section of the compression-absorption cascade cycle. However, it is clear that the first law analysis should be supported by the second law analysis for obtaining complete and detailed results. Therefore, the compression-absorption cascade cycles should also be investigated using the second law analysis for satisfactory results.

In this study, a second law analysis of compression-absorption cascade refrigeration cycles have been carried out, and separately, CO<sub>2</sub> has been included in the analysis for the vapor compression sections of the cascade cycle as refrigerant in order to compare its results with other refrigerants employed in the vapor compression section. First, R134a was considered in the vapor compression section of the cascade cycle along with LiBr-H<sub>2</sub>O or NH<sub>3</sub>-H<sub>2</sub>O fluid pairs in the absorption section in order to

choose the best suitable fluid pairs in the absorption section. Because LiBr-H<sub>2</sub>O fluid pair yielded better results, thermodynamic analyses were performed for different working temperatures of the system components by using only LiBr-H<sub>2</sub>O in the absorption section of cascade refrigeration system and various refrigerants, namely NH<sub>3</sub>, R134a, R410A and CO<sub>2</sub>, in the vapor compression section.

## DESCRIPTION AND ENERGY BALANCES OF THE CASCADE CYCLE

The base compression-absorption cascade refrigeration cycle which characterises totally five cycles investigated in this study is depicted in Figure 1. This cycle is very similar to classical cascade cycle that combines a serial form of vapor compressions cycle and absorption cycle. The absorption section of this cycle employs LiBr-H<sub>2</sub>O, while the vapor compression section employs R134a. Figures 2 and 3 show lnP-h and T-s diagrams of the single effect compression-absorption cascade refrigeration cycle, respectively.

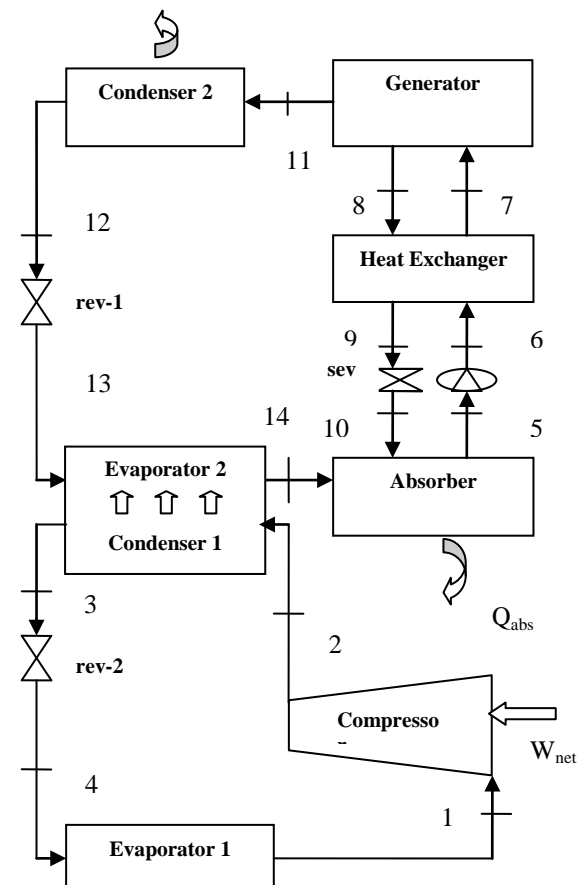


Figure 1. Schematic view of the single effect compression-absorption cascade refrigeration cycle.

A pump draws the weak LiBr solution from the absorber and forces it to pass through a heat exchanger. Then, the high-pressure cooled mixture leaves the exchanger and passes through the generator. After absorbing the heat applied to the generator, the water in the solution is driven out of it. Later, the strong LiBr solution leaving the generator undergoes a pressure drop

as it passes through a valve. Then, the solution goes to the absorber. In order to improve the performance of the cycle by increasing the temperature at state (6) and decreasing the temperature at state (9), an internal heat exchanger is used for energy recovering from strong solution to weak solution. After condensing by rejecting heat to the ambient, the cooling fluid (water) leaves the condenser as a saturated liquid. Then, the pressure of this stream is reduced by the expansion valve and directed to the evaporator, in which it absorbs the heat rejected in the condenser of the vapor compression section and evaporates. Then, this steam passes through the absorber and it is absorbed by hot solution. On the other hand, the refrigerant pressure is increased by the compressor in the vapor compression section, and the refrigerant is sent to the condenser. After condensing, the refrigerant pressure is dropped as it passes through the expansion valve. Then, the refrigerant is directed to the evaporator. The details of the base compression-absorption cascade refrigeration cycle can be found in Cimsit and Ozturk (2012)

The thermodynamic analysis of the cycles has been made based on the following assumptions:

1. The system operates in steady-state.
2. The states of the refrigerant at the outlets of the evaporator and condenser are saturated vapor and saturated liquid, respectively.
3. The weak refrigerant solution at the outlet of the absorber and strong solution at the outlet of the generator are saturated.
4. Pressure losses in the system components and lines are ignored.
5. In the absorption system, solution pump work input is negligible.
6. The isentropic efficiency of the compressor ( $\eta_s$ ) is 0.80, while its electric efficiency ( $\eta_e$ ) is 0.90.
7. The reference (or environment) temperature and pressure are assumed as 298K and 101.325 kPa, respectively, for exergy analysis.
8. The changes in the kinetic and potential energies are negligible.

The values of various parameters kept constant in the analysis are as follows:

$$T_{\text{evap}}=T_1=263\text{K}, T_{\text{con}}=T_{12}=313\text{K}, T_{\text{gen}}=363\text{K}, T_{\text{abs}}=313\text{K}, T_3=293\text{K} \text{ and } Q_{\text{evap1}}=50 \text{ kW.}$$

The mass, species and energy balance equations given below for steady state conditions can be applied to each system component.

$$\sum \dot{m}_i - \sum \dot{m}_e = 0 \quad (1)$$

$$\sum \dot{m}_i x_i - \sum \dot{m}_e x_e = 0 \quad (2)$$

$$\sum \dot{m}_i h_i - \sum \dot{m}_e h_e - \sum \dot{Q} - \dot{W} = 0 \quad (3)$$

The capacity of the components and circulation ratio in the absorption refrigeration section of the cascade cycle can be determined from the following equations:

$$\dot{Q}_{\text{con2}} = \dot{m}_{11}(h_{11} - h_{12}) \quad (4)$$

$$\dot{Q}_{\text{abs}} = \dot{m}_{10}h_{10} + \dot{m}_{14}h_{14} - \dot{m}_5h_5 \quad (5)$$

$$\dot{Q}_{\text{gen}} = \dot{m}_{11}h_{11} + \dot{m}_8h_8 - \dot{m}_7h_7 \quad (6)$$

$$\dot{Q}_{\text{evap2}} = \dot{m}_{13}(h_{14} - h_{13}) \quad (7)$$

$$f = \frac{\dot{m}_8}{\dot{m}_{11}} = \frac{x_7}{x_8 - x_7} \quad (8)$$

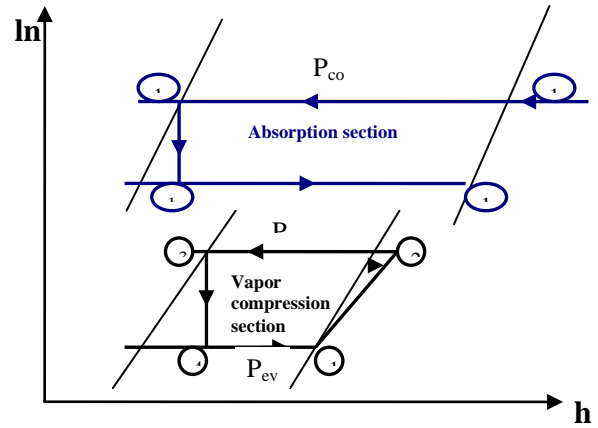


Figure 2. lnP-h diagram of the single effect compression-absorption cascade refrigeration cycle.

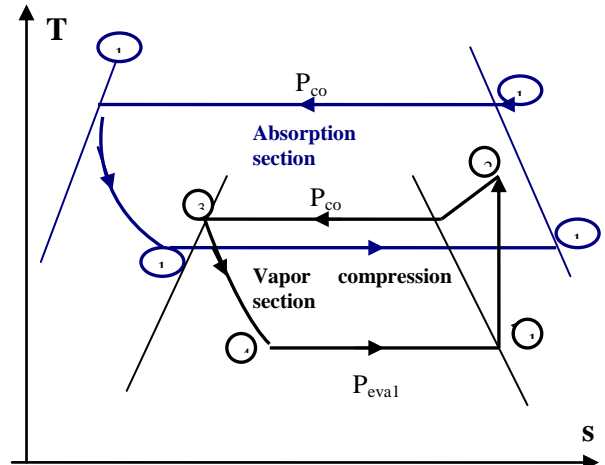


Figure 3. T-s diagram of the single effect compression-absorption cascade refrigeration cycle.

The capacity of the components in the vapor-compression refrigeration section of the cascade cycle can be determined from the following equations:

$$\dot{W}_{\text{comp}} = \dot{m}_1(h_2 - h_1) \quad (9)$$

$$\dot{Q}_{\text{con1}} = \dot{m}_3(h_2 - h_3) \quad (10)$$

$$\dot{Q}_{\text{evap1}} = \dot{m}_1(h_1 - h_4) \quad (11)$$

The COP for the overall the cascade cycle is defined as:

$$COP_{\text{cyclegen}} = \dot{Q}_{\text{evap1}} / (\dot{Q}_{\text{gen}} + \dot{W}_{\text{comp}}) \quad (12)$$

Details of the calculations of the thermodynamic properties can be found in Kaita (2001) and Ziegler (1984).

Referring to Figure 1, the operating conditions and thermodynamic properties at various points of the compression-absorption cascade refrigeration system are presented in Table 1, while R134a is used in the vapor-compression section for the sample cycle.

**Table 1.** Thermodynamic data and numerical values of the compression-absorption cascade refrigeration cycle for Figure 1

Poi nt	T (K)	$h$ (kJ/kg)	$s$ (kJ/kgK)	$\dot{m}$ (kg/s)	$x$ (LiBr %)
1	263	392.750	1.7337	0.2973	
2	298	417.719	1.7450	0.2973	
3	291	224.590	1.0865	0.2973	
4	263	224.590	1.0940	0.2973	
5	313	97.640	0.2560	0.2161	55
6	313	97.640	0.2560	0.2161	55
7	337	147.440	0.4042	0.2161	55
8	363	223.910	0.4882	0.1917	62
9	333	167.772	0.3332	0.1917	62
10	333	167.772	0.3332	0.1917	62
11	363	2670.00	8.5650	0.0244	
12	313	167.500	0.5723	0.0244	
13	283	167.500	0.5970	0.0244	
14	283	2518.90	8.8986	0.0244	

## THE SECOND LAW ANALYSIS OF THE CASCADE REFRIGERATION CYCLE

Exergy is defined as the maximum theoretical work that can be obtained from a system as it comes to equilibrium with the environment. The exergy balance equation for a control volume can be written as (Bejan *et al.* 1996):

$$\sum \dot{m}_i e_i - \sum \dot{m}_o e_o + \sum \dot{Q} \left(1 - \frac{T_0}{T}\right) - \sum \dot{W} - \dot{E}_D = 0 \quad (13)$$

The first two terms represent the sum of the time rates of exergy input and output of the system, respectively. The third term is the exergy transfer rate accompanying heat transfer.  $\dot{W}$  accounts for time rate of energy transfer by mechanical work, and  $\dot{E}_D$  is the time rate of exergy destruction due to irreversibilities within the control volume. If the changes in the kinetic and potential energies are neglected, the specific flow exergy can be evaluated from:

$$e = (h - h_0) - T_0(s - s_0) \quad (14)$$

The main sources of exergy destruction in a process are friction, heat transfer under finite temperature difference and unrestricted expansion (Talbi and Agnew, 2000). The rate of exergy destruction in each component of a compression-absorption cascade refrigeration cycle can be determined from:

$$\dot{E}_{D_{gen}} = \dot{m}_7 e_7 - \dot{m}_{11} e_{11} - \dot{m}_8 e_8 + \dot{Q}_{gen} \left(1 - \frac{T_0}{T_{gen}}\right) \quad (15)$$

$$\dot{E}_{D_{abs}} = \dot{m}_{10} e_{10} + \dot{m}_{14} e_{14} - \dot{m}_3 e_3 - \dot{Q}_{abs} \left(1 - \frac{T_0}{T_{abs}}\right) \quad (16)$$

$$\dot{E}_{D_{con2}} = \dot{m}_{11} e_{11} - \dot{m}_{12} e_{12} - \dot{Q}_{con} \left(1 - \frac{T_0}{T_{con2}}\right) \quad (17)$$

$$\dot{E}_{D_{she}} = \dot{m}_6 (e_6 - e_7) + \dot{m}_8 (e_8 - e_9) \quad (18)$$

$$\dot{E}_{D_{evap2}} = \dot{m}_2 (e_2 - e_3) + \dot{m}_{13} (e_{13} - e_{14}) \quad (19)$$

$$\dot{E}_{D_{evap1}} = \dot{m}_4 e_4 - \dot{m}_1 e_1 + \dot{Q}_{evap1} \left(1 - \frac{T_0}{T_{evap1}}\right) \quad (20)$$

$$\dot{E}_{D_{comp}} = \dot{m}_1 e_1 - \dot{m}_2 e_2 + \dot{W}_{comp} \quad (21)$$

$$\dot{E}_{D_{sev}} = \dot{m}_9 e_9 - \dot{m}_{10} e_{10} \quad (22)$$

$$\dot{E}_{D_{rev1}} = \dot{m}_{12} e_{12} - \dot{m}_{13} e_{13} \quad (23)$$

$$\dot{E}_{D_{rev2}} = \dot{m}_3 e_3 - \dot{m}_4 e_4 \quad (24)$$

The sum of the exergy destructions in the components of the cascade refrigeration cycle yields the total exergy destruction rate, i.e.:

$$\dot{E}_{Dt} = \sum_{i=1}^n \dot{E}_i \quad (25)$$

The exergetic efficiency ( $ECOP$ ), also called the second law efficiency, can be used to measure the performance of the cascade refrigeration cycle.  $ECOP$  is the ratio between the useful exergy obtained from a system and the useful exergy supplied to the system. In the cascade refrigeration cycle, while the exergy obtained from the system occurs with heat exchange between evaporator and ambient, the exergy supplied to the system occurs with heat exchange between generator and heat source and work provided by the compressor. Therefore, the exergetic efficiency can be written as:

$$ECOP = - \frac{\dot{Q}_{evap1} \left(1 - \frac{T_0}{T_{evap1}}\right)}{\dot{Q}_{gen} \left(1 - \frac{T_0}{T_{gen}}\right) + \dot{W}_{comp}} \quad (26)$$

## Second Law Thermodynamic Analyses Of The Cascade Refrigeration Cycles With LiBr/H<sub>2</sub>O-R134a And NH<sub>3</sub>/H<sub>2</sub>O-R134a

The energy and exergy analyses of the cascade refrigeration cycles have been performed for the cases of using LiBr-H<sub>2</sub>O and NH<sub>3</sub>-H<sub>2</sub>O in the absorption section and R134a in the vapor compression section of the cascade cycles. It is assumed that the input parameters are constant at  $T_1=263\text{K}$ ,  $T_{12}=313\text{K}$ ,  $T_3=291\text{K}$ ,  $T_{12}=363\text{K}$ , and cooling load is 50 kW.

The results of the energy and exergy analysis of the cycles are presented in Table 2. Moreover, it shows the



exergy destruction rates in the components and the total exergy destruction rate in the cycles. It is seen that the absorber causes the maximum exergy destruction rate, while the evaporator-1 causes quite low exergy destruction rate in comparison to other components. In the cycle using  $\text{NH}_3\text{-H}_2\text{O-R134a}$ , the components which cause the highest exergy destruction rate are the absorber, condenser-2 and generator in decreasing order.

**Table 2.** Exergy destruction rates in the components and performance of the cascade cycle

Components	LiBr/H <sub>2</sub> O-134a	NH <sub>3</sub> /H <sub>2</sub> O-134a
	$\dot{E}_D$ (kW)	$\dot{E}_D$ (kW)
Evaporator-1	0.053	0.053
Compressor	1.828	1.828
Evaporator- 2	2.023	1.438
Absorber	5.237	8.651
Solution heat exchanger	0.689	1.754
Generator	1.601	1.706
Condenser- 2	2.915	4.239
Exp.valve-1 (rev-1)	0.180	0.379
Exp.valve-2 (rev-2)	0.665	0.665
Total	15.191	20.713
Perform. of the cycle	LiBr/H <sub>2</sub> O-134a	NH <sub>3</sub> /H <sub>2</sub> O-134a
<i>ECOP</i>	0.304	0.242
<i>COP<sub>cyclegen</sub></i>	0.592	0.432

When LiBr-H<sub>2</sub>O fluid couple is used in the absorption section of cascade cycle, the *COP* is 27% higher and total exergy destruction rate is 20% lower from that obtained when  $\text{NH}_3\text{-H}_2\text{O}$  fluid couple is used. In both systems, the absorber causes the highest exergy destruction rate.

In this analysis, the exergy destruction rates were calculated for the cascade refrigeration given in Table 1, namely LiBr-H<sub>2</sub>O was accepted in the absorption section of cascade refrigeration system and R134a in the vapor compression section. Exergy destruction rates in the system components were presented for different working temperatures of the generator and evaporator. Figure 4 shows the highest values of the exergy destruction rates are observed in the absorber. It can be seen from Figure 4 that the exergy destruction rates of the absorber, condenser, generator and solution heat exchanger have a tendency to increase with increasing generator temperature. Also, the exergy destruction rates remain constant for the cascade heat exchanger, compressor and evaporator from the system elements.

Figure 5 shows that the exergy destruction rates decrease on increasing the evaporator temperature in the system components. The highest exergy destruction rates were obtained for the absorber, followed by condenser, and finally cascade heat exchanger.

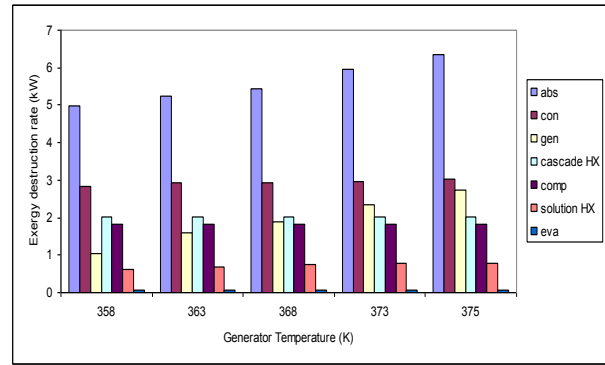


**Figure 4.** The change of exergy destruction rates as a function of generator temperature

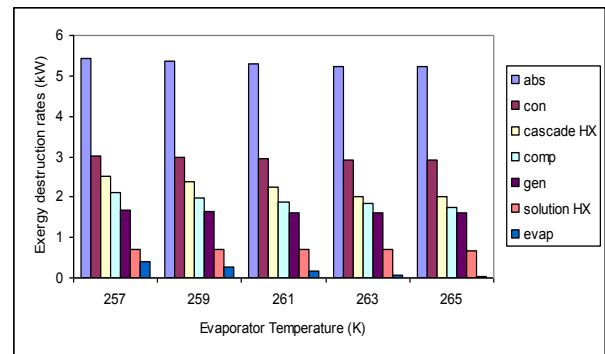


**Figure 5.** The change of exergy destruction rates as a function of evaporator temperature.

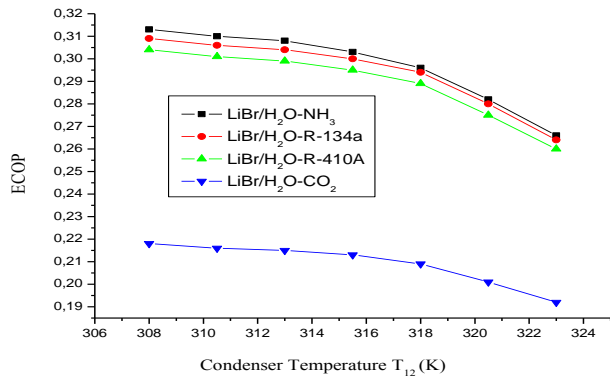
## RESULTS AND DISCUSSION

It has been determined that the use of LiBr-H<sub>2</sub>O fluid pair in the absorption section of the cascade cycle yields better results than  $\text{NH}_3\text{-H}_2\text{O}$  fluid pair in terms of the first and second law analyses. Therefore, the thermodynamic analyses were performed for different operating temperatures of the system components by using only LiBr-H<sub>2</sub>O in the absorption section and various refrigerants, namely  $\text{NH}_3$ , R134a, R410a and  $\text{CO}_2$ , in the vapor compression section of the cascade cycle. The results obtained from the analysis are given in Figures 6–18 for different operating temperatures of the cascade cycle.

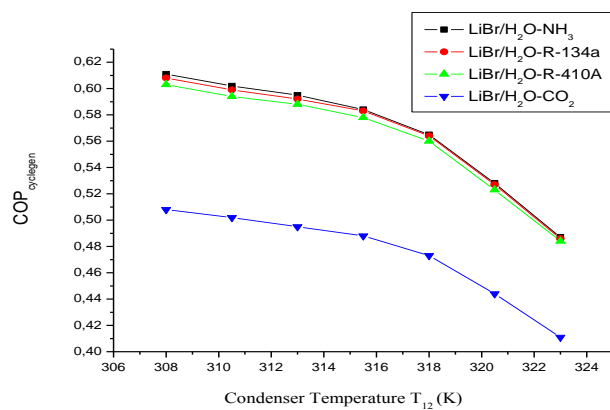
Figures 6 and 7 show the *COP<sub>cyclegen</sub>* and *ECOP*, respectively, as a function of condenser temperature for various refrigerants used in the vapor-compression section. As seen in these figures, the *COP<sub>cyclegen</sub>* and *ECOP* decrease on increasing the condenser temperature, as expected. This decrease is more obvious in the case of using  $\text{CO}_2$  in the vapor-compression section of the cascade cycle. The compressor power for the cascade cycle increases with increasing condenser temperature, thereby lowering *COP<sub>cyclegen</sub>*. Moreover, as the temperature difference between the condenser and the surrounding air increases due to increasing condenser temperature, the heat transfer in the condenser causes higher irreversibility, thus lowering exergetic efficiency of the cascade cycle.

Figure 8 shows that exergy destruction rates of the systems using  $\text{NH}_3$ , R134a and R410A are considerably

less than that using  $\text{CO}_2$  at increasing condenser temperatures.



**Figure 6.** The change of  $COP_{cyclegen}$  as a function of condenser temperature ( $T_{12}$ ).



**Figure 7.** The change of  $ECOP$  as a function of condenser temperature ( $T_{12}$ ).

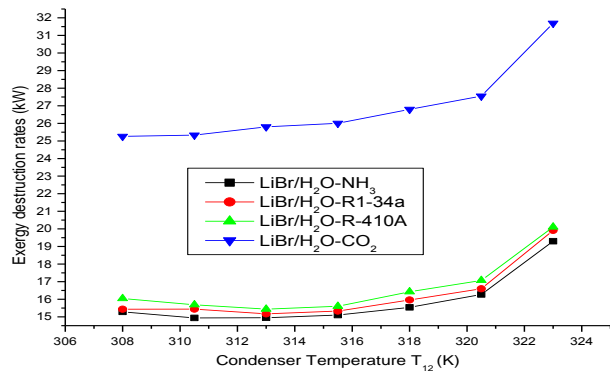


**Figure 8.** The change of exergy destruction rates (kW) as a function of condenser temperature ( $T_{12}$ ).

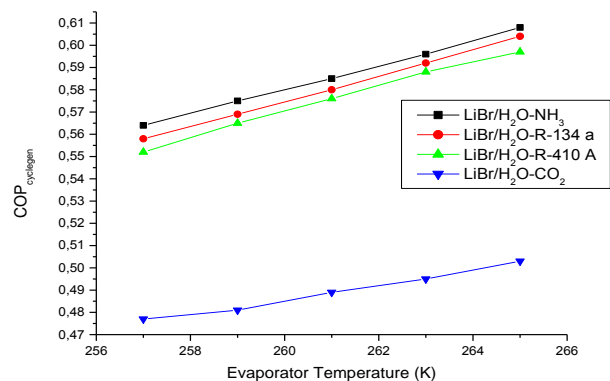


**Figure 9.** The change of  $COP_{cyclegen}$  as a function of evaporator temperature.

The changes of  $COP_{cyclegen}$  and  $ECOP$  with the evaporator temperature are presented in Figures 9 and 10, respectively, for various refrigerants used in vapor compression section. As shown in Figure 9,  $COP_{cyclegen}$  increases with increasing evaporator temperature of the cycle. When the evaporator temperature and pressure increase, the compression ratio of the vapor compression section decreases. Therefore, the temperature difference between the cascade heat exchanger and the evaporator decreases, which leads to decreasing compressor power and increasing  $COP$ . The exergetic efficiency for the cascade system decreases with increasing evaporator temperature, as indicated in Figure 10. The compressor power and the exergy flow rate of evaporator decrease with increasing evaporator temperature, thus decreasing  $ECOP$ .

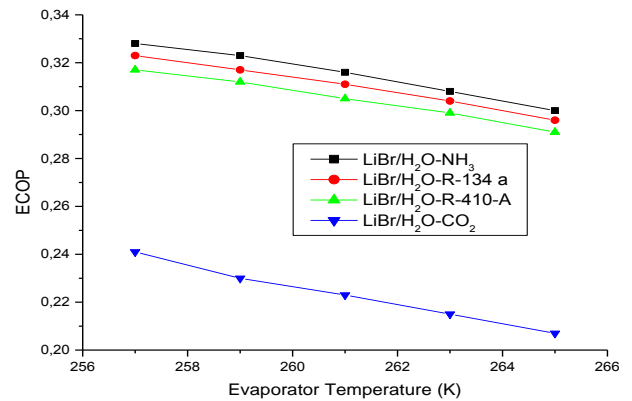


**Figure 10.** The change of  $ECOP$  as a function of evaporator temperature

Figures 11 and 12 present the  $COP_{cyclegen}$  and  $ECOP$ , respectively, as a function of generator temperature for various refrigerants used in vapor-compression section. As seen in Figure 11, the  $COP_{cyclegen}$  increases on increasing the generator temperature of the cycle. The maximum  $COP$  is obtained at 368K generator temperature. It is seen in Figure 12 that the higher the generator temperature, the lower the  $ECOP$ . Because the generator needs more external thermal energy input to the system at higher generator temperatures, the irreversibility in the generator increases with rising generator temperatures. The other irreversibility source of the generator is the mixing process. The mixing irreversibility is associated with the evaporation of the refrigerant in the generator from the solution. The concentrated solution requires a greater amount of heat to evaporate it in a pure state, and consequently, the  $ECOP$  of the cascade system decreases. Ammonium has a better performance among four refrigerants for vapor compression section of the cascade cycle. On other hand,  $\text{CO}_2$  has the poorest performance as seen in Figure 12.

Figure 13 shows that the highest values of the exergy destruction rates occur at the high generator temperatures. The highest values of exergy destruction rates are observed with  $\text{LiBr}/\text{H}_2\text{O}-\text{CO}_2$ , and lower values are obtained with  $\text{R134a}-\text{LiBr}/\text{H}_2\text{O}-\text{NH}_3$ .

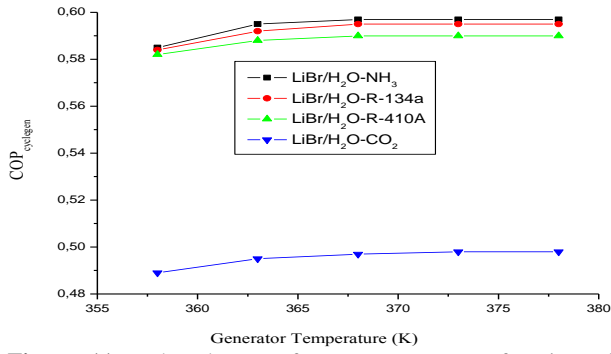


**Figure 11.** The change of  $COP_{cyclegen}$  as a function of generator temperature.

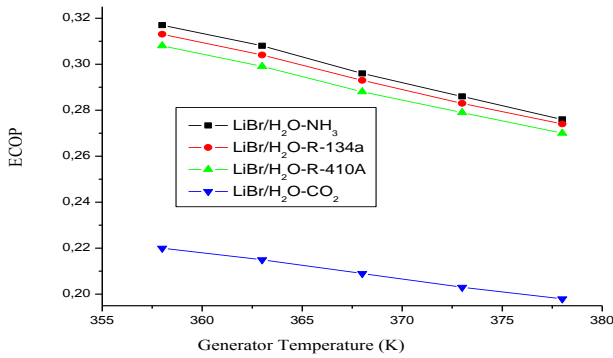


**Figure 12.** The change of  $ECOP$  as a function of generator temperature.

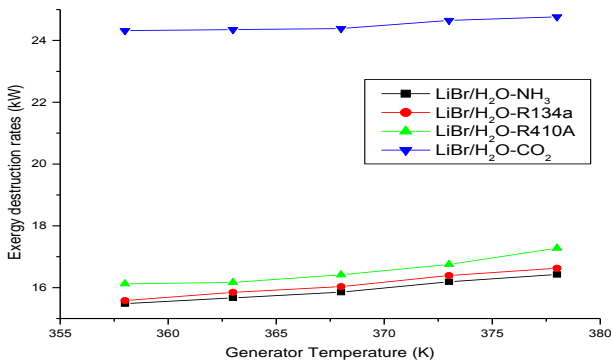
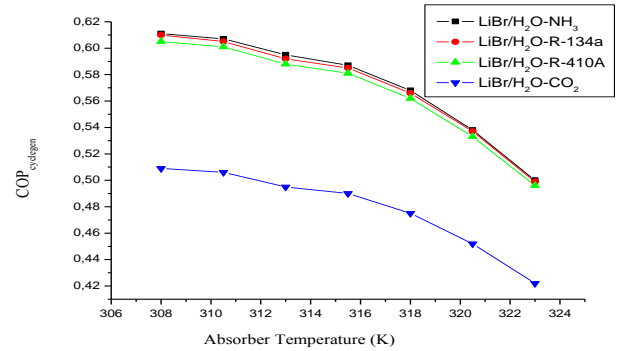


**Figure 13.** The change of exergy destruction rates (kW) as a function of generator temperature.

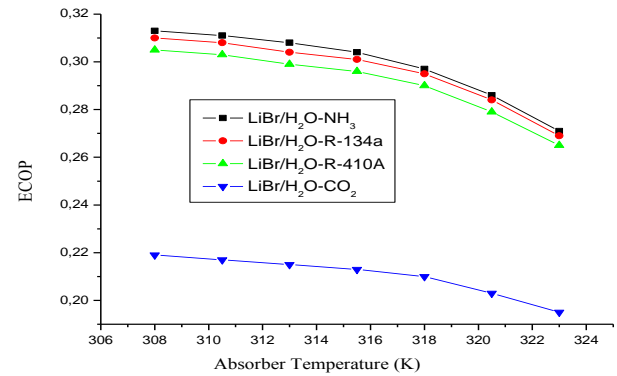
The changes of  $COP_{cyclegen}$  and  $ECOP$  with absorber temperature are presented in Figures 14 and 15, respectively, for various refrigerants used in vapor compression section. Since the generator needs more external thermal energy input to the system, extra cooling is needed in the condenser and absorber. Moreover, because the absorber involves the mixing of the fluids with different phase and temperature mixing process, and consequently, the absorber causes the highest exergy destruction rate in the cascade cycle. The  $COP$  and  $ECOP$  for the cascade system decrease with increasing absorber temperatures, as indicated in Figures 14 and 15, respectively.

Similar to the condenser, the absorber is generally cooled by ambient air. Rising absorber temperature increases the temperature difference between the fluid pair and the ambient, therefore causing a higher irreversibility due to the heat transfer occurring at a high temperature difference. Figure 16 indicates that the

exergy destruction rates of the cascade cycle increase with increasing absorber temperatures. The cascade cycle using  $LiBr/H_2O-CO_2$  yields the highest exergy destruction rates compared with other fluids.

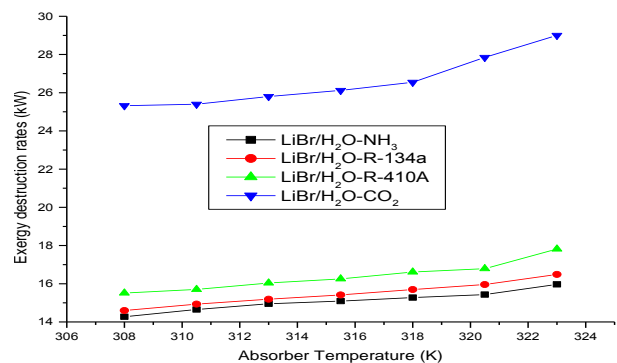


**Figure 14.** The change of  $COP_{cyclegen}$  as a function of absorber temperature.



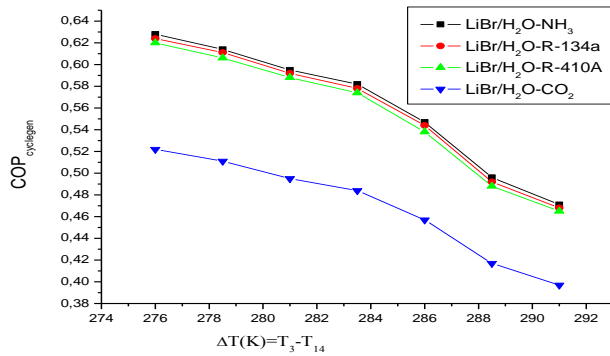
**Figure 15.** The change of  $ECOP$  as a function of absorber temperature.

Figure 17 and 18 present the  $COP_{cyclegen}$  and  $ECOP$ , respectively, as a function of temperature differences of the cascade heat exchanger. The temperature difference in the cascade heat exchanger ( $\Delta T$ ) is taken as the temperature difference between the evaporator temperature of the absorption section and the condenser temperature of the vapor compression section of the cascade cycle. In this analysis, the evaporator temperature ( $T_{14}$ ) of the absorption refrigeration section of cascade cycle is varied between 278K and 288K with increments of 2.5K. It can be seen in Figures 17 and 18 that the  $COP_{cyclegen}$  and  $ECOP$  for the compression-absorption cascade refrigeration cycle decrease with increasing temperature difference  $\Delta T$  ( $T_3-T_{14}$ ).



**Figure 16.** The change of exergy destruction rates (kW) as a function of absorber temperature.





**Figure 17.** The change of  $COP_{cyclegen}$  as a function of  $\Delta T$  temperature differences.

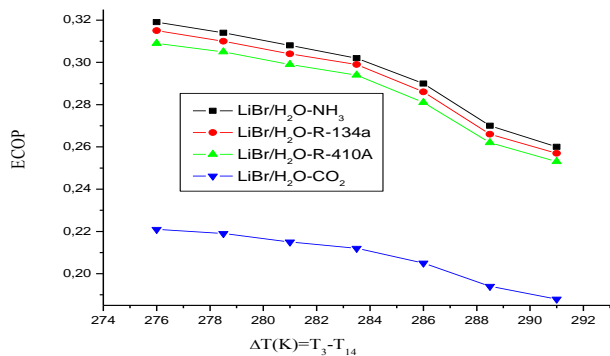


**Figure 18.** The change of  $ECOP$  as a function of  $\Delta T$  temperature differences

## CONCLUSIONS

The first and second law analyses of the compression-absorption cascade refrigeration cycles have been carried out for the case of using LiBr-H<sub>2</sub>O fluid pair in the absorption section of the cascade cycle, and the results were compared with using NH<sub>3</sub>-H<sub>2</sub>O pair. When LiBr-H<sub>2</sub>O fluid pair is used in the absorption section of the cascade cycle, the  $COP$  is 27% higher than the case of using NH<sub>3</sub>-H<sub>2</sub>O fluid pair for a sample application. In the case of using LiBr-H<sub>2</sub>O fluid couple in the absorption section of the cascade refrigeration systems, the total exergy destruction rate is 20% lower than that obtained in the case of NH<sub>3</sub>-H<sub>2</sub>O fluid couple. In both systems, the highest exergy destruction rates occur in the generator, condenser and absorber in decreasing order. By focusing attention on the components causing high exergy destructions, the total exergy destruction rate in the system can be decreased, and the  $COP$  of the system can be improved.

Because better results were obtained with LiBr-H<sub>2</sub>O fluid pair, energy and exergy analysis has been performed for different working temperatures of the system components by using only LiBr-H<sub>2</sub>O in the absorption section of cascade refrigeration system and different refrigerants (NH<sub>3</sub>, R134a, R410A and CO<sub>2</sub>) in the vapor compression section. Increasing the generator and evaporator temperatures promotes the  $COP$  of the cascade cycle, while increasing the condenser and absorber temperatures decreases it. The exergetic efficiency of the system decreases on increasing the generator, absorber and condenser temperatures. The total irreversibility of the cascade heat exchanger

increases with increasing temperature difference  $\Delta T$  ( $T_3-T_{14}$ ), thereby decreasing the exergetic efficiency of the system. The highest  $COP_{cyclegen}$  and  $ECOP$  values have been obtained from the refrigerants NH<sub>3</sub>, R134a, R410A and CO<sub>2</sub>, in decreasing order, used in the vapor compression section. Ammonium has a better performance among four refrigerants for vapor compression section of the cascade cycle. The performance of R134a is found to be very similar to that of NH<sub>3</sub>. On other hand, CO<sub>2</sub> has the poorest performance. These refrigerants are seen to be the preferred refrigerants when environmental factors are also considered as they have the lowest ozone depletion potential. Furthermore, LiBr-H<sub>2</sub>O/ NH<sub>3</sub> vapor compression-absorption cascade cycle has the highest but LiBr-H<sub>2</sub>O/CO<sub>2</sub> vapor compression-absorption cascade cycle has the lowest first and second law performance with a substantial difference between them.

Cooling systems require novel refrigeration cycles to be used for energy savings. Especially compression-absorption cascade refrigeration systems can be considered as alternative to vapor compression refrigeration systems. Because these cycles provide cooling by utilizing the thermal energy such as waste heat, geothermal or solar heat, the electrical energy required for the cascade cycle is less than vapor compression cycle. Also, these cycles operate on environmentally-friendly refrigerants.

In order to increase the performance and decrease the investment and operating costs of the cascade cycles, special attention must be given to the components having high exergy destruction rates, and cost aided thermodynamic analysis, also called thermo-economic analysis, can be applied to these cascade cycles as a further study.

## REFERENCES

- Joudi, K.A., Lafta, A. H., 2001, Simulation of a simple absorption refrigeration system, *Energy Conversion and Management*, 42, 1575-1605.
- Florides, G.A., Tassou, S.A., Kalogirou, S.A., Wrobel, L.C., 2003, Design and construction of a LiBr-water absorption machine, *Energy Conversion and Management*, 44, 2483-2508.
- Sozen, A., 2001, Effect of heat exchangers on performance of absorption refrigeration systems, *Energy Conversion and Management*, 42, 1699-1716.
- Talbi, M., Agnew, B., 2000, Exergy analysis: an absorption refrigerator using lithium bromide and water as the working fluids, *Applied Thermal Engineering*, 20, 619-630.
- Adewusi, S.A., Zubair, S.M, 2004, Second law based thermodynamic analysis of ammonia-water absorption systems, *Energy Conversion and Management*, 45, 2355-2369.

Sencan, A., Yakut, K.A., Kalogirou, S.A., 2005, Exergy analysis of lithium bromide/water absorption systems, *Renewable Energy*, 30, 645-657.

Kilic, M., Kaynakli, O., 2007, Second law-based thermodynamic analysis of water lithium bromide absorption refrigeration system, *Energy*, 32, 1505-1512.

Kaynakli, O., Yamankaradeniz, R., 2007, Thermodynamic analysis of absorption refrigeration systems based on entropy generation, *Current Science*, 92, 4, 472-479.

Kaynaklı, O., Kilic, M., 2007, Theoretical study on the effect of operating conditions on performance of absorption refrigeration system, *Energy Conversion and Management*, 48, 599-607.

Kaushik, S.C., Arora, A., 2009, Energy and exergy analysis of single effect and series flow double effect water-lithium bromide absorption refrigeration systems, *Int. J. Refrigeration*, 32, 1247-1258.

Rivera, W., Cerezo, J., Martinez, H., 2010, Energy and exergy analysis of an experimental single-stage heat transformer operating with the water/lithium bromide mixture, *Int. J. Energy Res.*, 34, 1121-1131.

Misra, R.D., Sahoo, P.K., Sahoo, S., Gupta, A., 2003, Thermoeconomic optimization of a single effect

water/LiBr vapour absorption refrigeration system, *Int. J. Refrigeration*, 26, 158-169.

Tarique, S., Siddiqui, M., 1999, Performance and economic study of the combined absorption/compression heat pump, *Energy Conversion and Management*, 40, 575-591.

Kairouani, L., Nehdi, E., 2006, Cooling performance and energy saving of compression-absorption refrigeration system assisted by geothermal energy, *Applied Thermal Engineering*, 26, 288-294.

Cimsit, C., Ozturk, I.T., 2012, Analysis of compression-absorption cascade refrigeration cycles, *Applied Thermal Engineering*, 40, 311-317.

Kaita, Y., 2001, Thermodynamic properties of lithium bromide-water solutions at high temperatures, *International Journal of Refrigeration*, 24, 374-390.

Ziegler, B., Trepp, Ch., 1984, Equation of state for ammonia-water mixtures, *International Journal of Refrigeration*, 7, 2, 101-6.

Bejan, A., Tsatsaronis, Moran, G., M., 1996, Thermal design and optimization. New York: John Wiley and Sons Inc; 1996.

### **Yrd. Doç. Dr. Canan CİMŞİT**

İlk, orta ve lise eğitimini Kocaeli tamamladı. Karadeniz Teknik Üniversitesi Mühendislik-Mimarlık Fakültesi Makine Mühendisliği Bölümü'nden mezun oldu. Kocaeli Üniversitesi Fen Bilimleri Enstitüsü'nde yüksek lisansını tamamladı. Kocaeli Üniversitesi Fen Bilimleri Enstitüsü Makina Mühendisliği Anabilim Dalı'ndan Doktora derecesini aldı. Halen Kocaeli Üniversitesi Gölcük Meslek Yüksekokulu'nda öğretim üyesi olarak çalışmaktadır.

### **Prof. Dr. İlhan Tekin ÖZTÜRK**

Yıldız Üniversitesi Kocaeli Mühendislik Fakültesi Makine Mühendisliği Bölümü'nden 1985 yılında mezun oldu. Yine aynı üniversitenin Fen Bilimleri Enstitüsü'nde 1987 yılında yüksek lisansını tamamladı. 1993 yılında Y.T.Ü. Fen Bilimleri Enstitüsü Makina Mühendisliği Anabilim Dalı'ndan Doktora derecesini aldı. 1998 yılında Makina Mühendisliği Termodinamik Anabilim Dalı'ndan Doçent ve 2004 tarihinde yine aynı anabilim dalından Profesör unvanını aldı. 1987-1992 tarihleri arasında YTÜ Kocaeli Mühendislik Fakültesi Makine Mühendisliği Bölümü'nde araştırma görevlisi olarak görev yaptı. 1993 tarihinden itibaren Kocaeli Üniversitesi Mühendislik Fakültesi Makine Mühendisliği Bölümü Termodinamik ve Isı Tekniği Anabilim Dalı'nda öğretim üyesi olarak görevine devam etmektedir. Evli ve bir çocuk babası olan ÖZTÜRK'ün uzmanlık alanları; Termodinamik, Ekserji Analizi, Termoeconomik Optimizasyon, Enerji Yönetimi, Bölgesel Isıtma, İklimlendirme, Soğutma ve Yalıtım olarak sıralanabilir. TMMOB Makine Mühendisleri Odası, Türk Isı Bilimi ve Tekniği Derneği ve Türk Tesisat Mühendisleri Derneği üyesidir.

### **Prof. Dr. Murat HOŞÖZ**

Uludağ Üniversitesi Mühendislik Fakültesi Makine Mühendisliği Bölümü'nden 1988 yılında lisans derecesini, İstanbul Teknik Üniversitesi Fen Bilimleri Enstitüsü Makine Mühendisliği Anabilim Dalı'ndan sırasıyla 1990 yılında yüksek lisans ve 1999 yılında doktora derecelerini aldı. Uludağ Üniversitesi Mühendislik Fakültesi Makine Mühendisliği Bölümü'nde 1989-1991 yılları arasında Araştırma Görevlisi olarak çalıştı. 1991-1999 yılları arasında Kocaeli Üniversitesi Kocaeli Meslek Yüksekokulu İklimlendirme-Soğutma Programı'nda Öğretim Görevlisi olarak görev yaptı. 1999-2006 yılları arasında Kocaeli Üniversitesi Teknik Eğitim Fakültesi Makine Eğitimi Bölümü'nde Yardımcı Doçent, 2006-2011 yılları arasında aynı bölümde Doçent olarak çalıştı. 2012 yılından bu yana, Kocaeli Üniversitesi Teknoloji Fakültesi Otomotiv Mühendisliği Bölümü'nde Profesör olarak görev yapmaktadır. Soğutma ve iklimlendirme sistemleri, taşıt iklimlendirmesi ve içten yanmalı motorların termodinamik analizi üzerine çalışmaları bulunmaktadır.